# AJNR

# MR Imaging of Hemorrhagic Intracranial Neoplasms

Sylvie Destian, Gordon Sze, George Krol, Robert D. Zimmerman and Michael D. F. Deck

This information is current as of July 5, 2025.

# MR Imaging of Hemorrhagic Intracranial Neoplasms

Sylvie Destian[1]
Gordon Sze[2]
George Krol[2]
Robert D. Zimmerman[1]
Michael D. F. Deck[1]

Thirty patients with intracranial tumors containing hemorrhage of varying stages were examined with high-field-strength MR imaging and CT to determine what differences might exist between hemorrhagic tumor and pure hemorrhage. Pathology was obtained in the six patients with primary tumors and in 14 of the 24 patients with metastases. Similar to evolving intraparenchymal hematomas, hemorrhagic neoplasms undergo changes in their appearance that can be categorized into three distinct intensity patterns, or stages. Stage 1 is characterized as iso- or hypointensity on short TR sequences and as hypointensity on long TR sequences; stage 2 as developing hyperintensity on both short and long TR sequences, without evidence of a well-defined black rim; and stage 3 as a hyperintense lesion with a well-defined black rim on long TR sequences. An additional mixed-intensity pattern was identified, which contained areas corresponding to more than one stage. In all of the cases exhibiting this pattern, pathology confirmed that the appearance was due to recurrent bleeding. We found several characteristics on MR that, when present, suggest an underlying neoplasm. These include delay in evolution between stages, central or eccentric hyperintensity in stage 2, and a mixed-intensity pattern. In addition, the presence of a hemosiderin rim does not exclude an underlying neoplasm.

We found that the MR patterns that characterize hemorrhagic intracranial neoplasms should help to determine the cause of the hemorrhage.

During the past few years MR imaging has emerged as superior to CT in detecting intraparenchymal hemorrhage, particularly in the subacute and chronic phases. In addition, it is an excellent, noninvasive way to screen for, and follow, intracranial neoplasms. In patients who present with a hemorrhage on MR, however, it may be necessary to determine the underlying cause of hemorrhage.

Recently, several reports have described the MR characteristics of intraparenchymal hemorrhage [1–11]. However, only a few studies describing the MR characteristics of hemorrhagic neoplasms have been reported in the literature [11–15]. Therefore, we examined patients with hemorrhagic neoplasms to determine whether there were any differences in the appearance of the lesions on MR that would distinguish them from pure hemorrhage.

## Materials and Methods

Thirty patients with hemorrhagic intracranial neoplasms were examined by MR and CT. There were 22 men and eight women, ranging in age from 20 to 72 years old. Six of the patients had primary tumors and 24 had metastatic tumors. Pathology was obtained in all six patients with primary tumors and in 14 of the patients with metastases. The primary tumors included two gliomas, two meningiomas, an ependymoma, and a primary meningeal melanoma. The metastatic tumors included 12 of melanoma, two of lung, two of renal cell, two of colon, and one each of bladder, thyroid, testicular, endometrial, rhabdomyosarcoma, and extragonadal choriocarcinoma.

All patients were examined on a 1.5-T GE superconducting magnet using short TR, 600–800/20–25/2 (TR range/TE range/excitations), and multiecho long TR, 2000/35–80/2, spin-

echo sequences. The images were acquired on a 256 × 256 or 256 × 128 matrix with a 5-mm slice thickness. The interslice gap was 1 mm for the short TR sequences and 2.5 mm for the long TR sequences. In addition, each patient had a noncontrast and a contrast CT scan, which were performed on a fourth-generation scanner with contiguous 5–10-mm-thick slices, either the same day or within 3 days of the MR imaging. The age of the hemorrhage was determined by the clinical history and the CT findings, and then correlated with the appearance on MR.

Six of the patients with metastatic disease had a follow-up examination at least once, and in one case five times. Three of the patients had more than one examination prior to their initial surgery. The other three patients developed new lesions after initial resection and were followed untreated for their new brain metastases, or had resection of a new lesion. The stage of each lesion was determined by its appearance on the first examination.

All of the surgical specimens were subjected to routine gross and microscopic pathologic examination. Five of the seven excised melanoma metastases, however, were found to be heavily pigmented on microscopic examination with hematoxylin and eosin. Therefore, special staining techniques were employed for these five specimens to determine whether the hyperpigmentation was due to melanin, hemosiderin, or both. A Fontana Masson stain was done to detect melanin and an iron stain was done to detect hemosiderin.

## Results

We found that hemorrhagic neoplasms undergo changes in their appearance that can be categorized into three distinct intensity patterns. These intensity patterns, however, are only somewhat time-dependent in that they do not always correlate with the clinical time course of the neoplastic hemorrhage, as they do with pure hemorrhage. The conventional terms used to describe the age-related signal intensity patterns of pure hemorrhage—i.e., acute, subacute and chronic—are not really appropriate when referring to neoplastic hemorrhage, because the time of evolution of the latter is variable. Therefore, rather than using the conventional nomenclature, which may be misleading, we defined the intensity patterns of our lesions as stages 1, 2, and 3. Table 1 is a summary of the findings in 24 of our patients as compared with findings in pure hemorrhage. A stage-1 lesion (Fig. 1) is isointense or mildly hypointense on short TR sequences and hypointense on long TR sequences. Seven of the patients had stage-1 lesions. Included in this group were one patient with a meningioma, two patients with metastatic melanoma, and one patient each with metastatic bladder, metastatic rectal, and metastatic colon carcinoma. Stage-2 lesions (Fig. 2) develop hyperintensity on both short and long TR sequences. Of the six patients in this group, one patient had an astrocytoma, three patients had metastatic melanoma, and the other two patients had metastatic endometrial and metastatic testicular carcinoma. Stage-3 lesions (Fig. 3) are hyperintense on both short and long TR sequences with a well-defined black rim on the long TR sequence. Eleven patients had stage-3 lesions. One of these patients had a meningioma, one had a primary meningeal melanoma, four had metastatic melanoma, two

**TABLE 1: Signal Intensity Patterns of Hemorrhagic Neoplasms Compared with Described Evolution of Pure Hemorrhage**

| Hemorrhagic Neoplasm | | Signal Intensity | | Pure Hemorrhage | |
|---|---|---|---|---|---|
| Stage | Age | Short TR | Long TR | Stage | Age |
| 1 | Variable | Iso, Hypo | Hypo | Acute | 2–5 days |
| 2 | Variable | Iso→Hyper | Iso→Hyper | Subacute | 5–14 days |
| 3 | Variable | Hyper | Hyper with black rim | Chronic | 2 wk–mos |
| M | Variable | Variable | Variable | | |

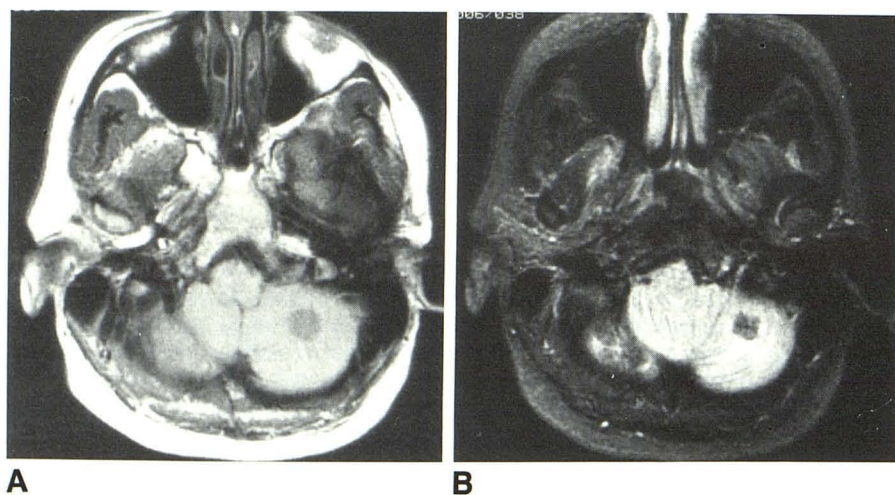

**A**                    **B**

Fig. 1.—A and B, Colon metastases, left cerebellum; stage 1. Lesion is mildly hypointense on short TR sequence (600/20) (A) and markedly hypointense on long TR sequence (2000/70) (B).

Fig. 2.—A and B, Testicular metastasis, right cerebellum; stage 2. Lesion contains eccentric hyperintensity (*solid arrows*) representing free methemoglobin on both short TR (600/20) (A) and long TR (2000/70) (B) sequences. Isointense area on short TR sequence, which is hypointense on long TR sequence (*open arrows*), represents residual stage-1 hemorrhage.



A                B
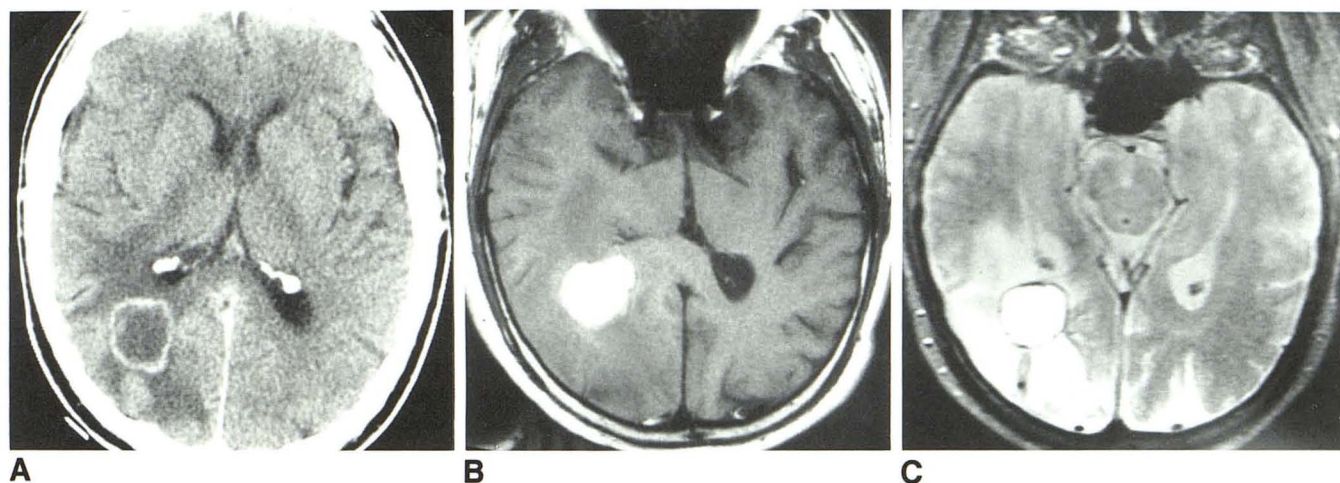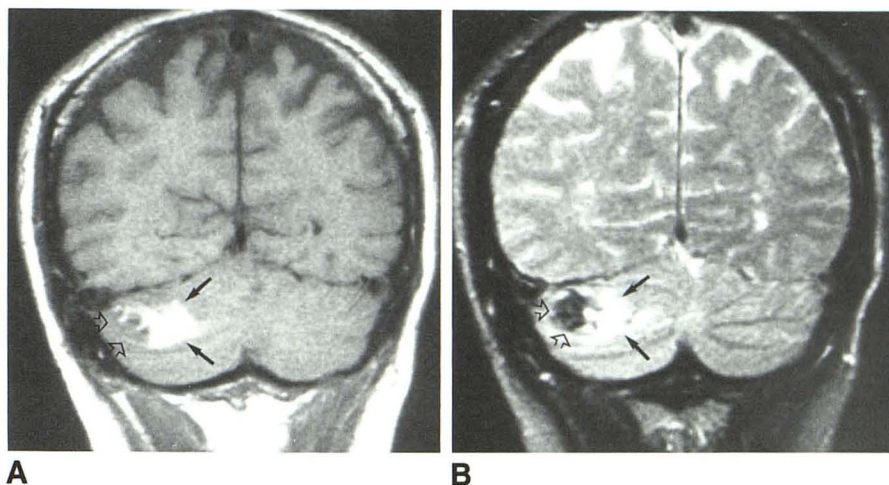


A                B                C

Fig. 3.—A–C, Renal cell metastasis, right occipital lobe; stage 3. Contrast CT scan (A) shows ring-enhancing hypodense mass in right occipital lobe. Lesion is hyperintense on both short TR sequence (600/20) (B) and long TR sequence (2000/70) (C) with a well-defined thin hypointense rim apparent on long TR image.

had metastatic lung, two had metastatic renal cell, and one had metastatic choriocarcinoma. Additionally, six patients exhibited a fourth intensity pattern, which we defined as mixed (Fig. 4). Those lesions demonstrating a mixed-signal-intensity pattern contained areas corresponding to more than one of the three stages described above. Three of the mixed lesions (metastatic melanoma, metastatic rhabdomyosarcoma, and glioblastoma multiforme) contained stage-1 and stage-2 elements. Two of the mixed lesions (ependymoma and metastatic melanoma) contained elements of all three stages, and the sixth mixed lesion (metastatic thyroid) contained stage-2 and stage-3 elements.

On noncontrast CT, five of the stage-1 lesions were hyperdense and two were mildly hyperdense. Two of the stage-2 lesions were isodense, one was mildly hyperdense, and three were hyperdense. Five of the stage-3 lesions were hypodense, four were isodense, and two were mildly hyperdense.

All of the mixed-stage lesions appeared inhomogeneous, containing areas of hypo- iso-, and hyperdensity (Fig. 4A). After the administration of IV contrast material, the five hyperdense stage-1 lesions did not demonstrate appreciable enhancement, but the two mildly hyperdense stage-1 lesions enhanced homogeneously. The two stage-2 lesions that were isodense on noncontrast CT demonstrated ring enhancement after contrast administration; the other four enhanced homogeneously. Four of the five hypodense stage-3 lesions demonstrated ring enhancement (Fig. 3A), and one did not enhance. The other six stage-3 lesions demonstrated homogeneous enhancement. All of the mixed-stage lesions enhanced inhomogeneously (Fig. 4B).

Histopathology was available in five of the patients with stage-1 lesions, one of the patients with a stage-2 lesion, eight of the patients with stage-3 lesions, and all of the patients with mixed lesions. All of the stage-1 lesions con-
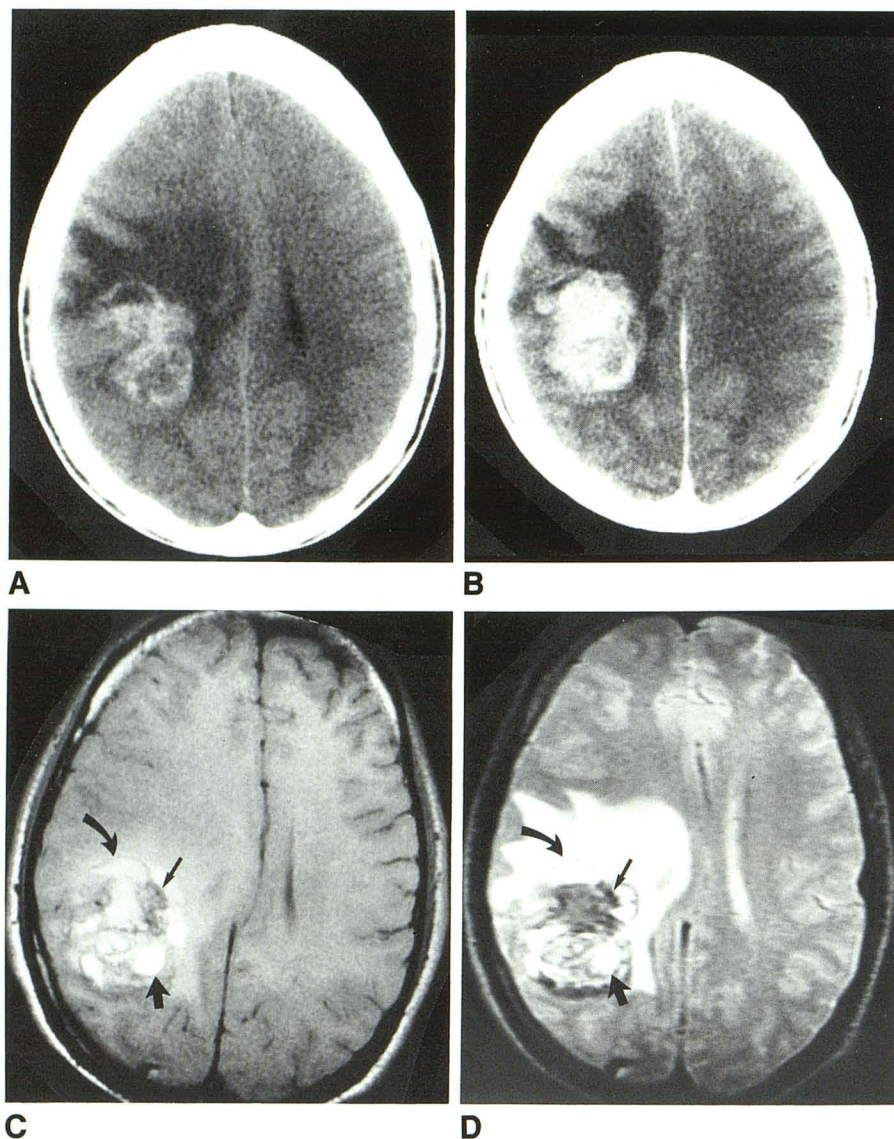
A

B





C

D

Fig. 4.—A–D, Melanoma metastasis, right frontoparietal region; mixed signal intensity. Noncontrast CT scan (A) shows inhomogeneous mass with areas of hypo- and hyperdensity. Contrast CT scan (B) (obtained at slightly higher level) demonstrates areas of enhancement within lesion. On short TR (800/20) (C) and long TR (2000/70) (D) sequences, lesion contains areas corresponding to stage-1 hemorrhage (small arrows), stage-2 hemorrhage (large arrows), and stage-3 hemorrhage (curved arrows).

tained fresh hemorrhage on histologic examination. The stage-2 lesion contained organizing hemorrhage without evidence of hemosiderin, and the stage-3 lesions contained old hemorrhage and hemosiderin. In each of the mixed lesions pathology demonstrated areas of hemorrhage in different stages of evolution, corresponding to the stages seen on MR. The stages of those lesions without pathology were determined by their appearance on MR and confirmed by the clinical history and the appearance of the lesions on CT.

Although there was direct correlation between the stage of the hemorrhagic component of the lesions on MR and what was seen pathologically, the intensity pattern of the hemorrhagic neoplasms did not necessarily reflect the clinical age of the hemorrhage. While in some cases the time course of evolution was similar to pure hemorrhage, in other cases there was a delay in evolution between stages. Of the four

patients who were examined serially, three had a lesion or lesions that exhibited delayed evolution. The most dramatic example (Fig. 5) occurred in a patient who was followed over several months before treatment was begun for her hemorrhagic supratentorial colon metastases, which developed after resection of three hemorrhagic posterior fossa metastases. On the initial scan the lesion was hypointense on both short and long TR sequences, corresponding to a stage-1 lesion. One month later the lesion was still hypointense on both short and long TR sequences, in contrast to what one would expect to see in a pure hemorrhage. Two months after the initial examination, however, the lesion began to develop some hyperintensity.

Another significant difference in the appearance of hemorrhagic neoplasms is seen in stage-2 lesions. While in pure subacute intraparenchymal hemorrhage the hyperintensity
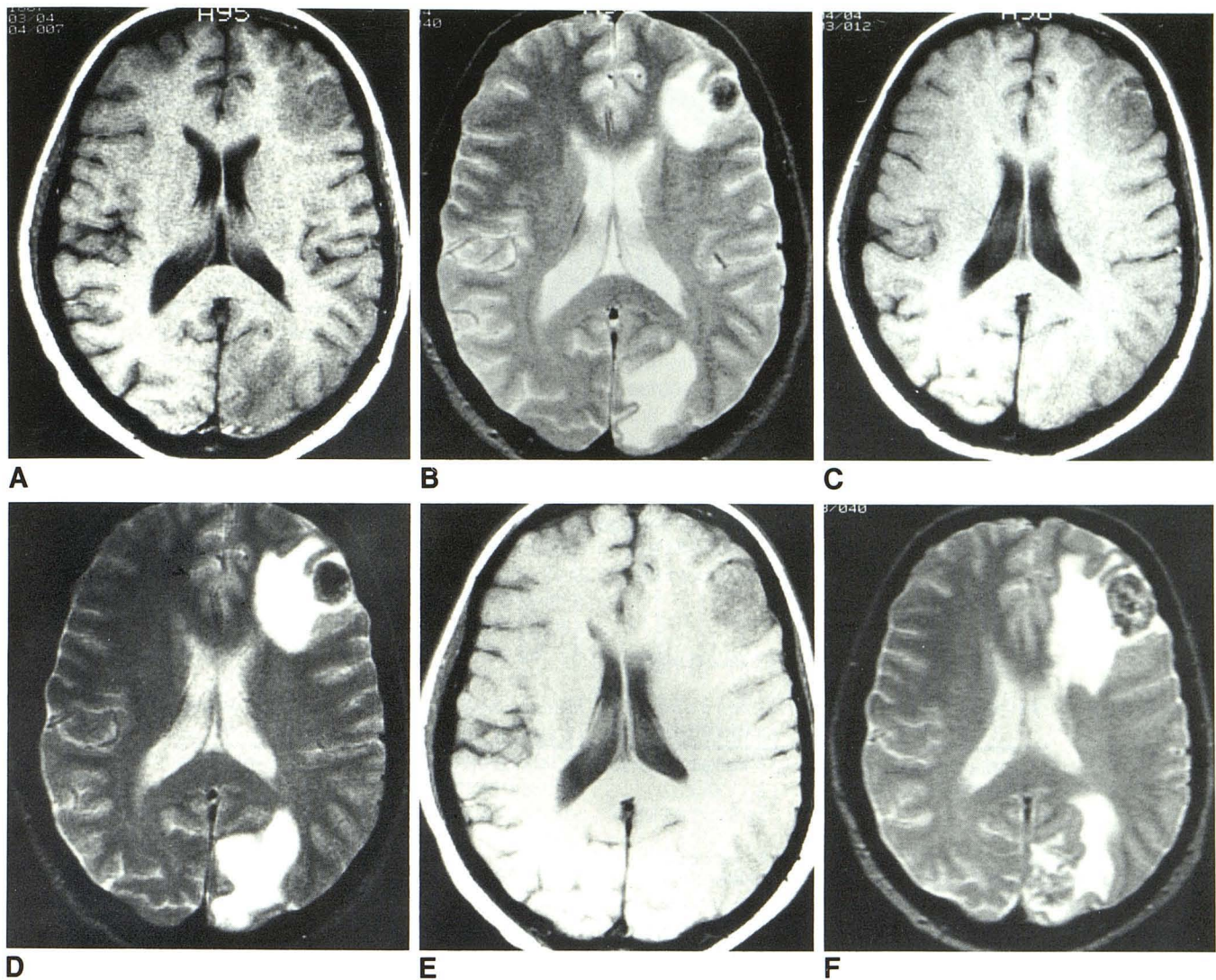
Fig. 5.—A–F, Colon metastasis, left frontal lobe; delayed evolution. Initial examination showed mildly hypointense lesion on short TR sequence (600/20) (A), which became markedly hypointense with surrounding edema on long TR sequence (2000/70) (B). Edema surrounding a small lesion was also seen in left occipital lobe. One month after initial examination, frontal lobe lesion appeared larger, but signal intensity characteristics were unchanged on short TR (800/20) (C) and long TR (2000/70) (D) sequences. Two months after initial examination, frontal lobe lesion appeared larger and less hypointense on short TR sequence (800/20) (E) and had developed irregular central hyperintensity on long TR sequence (2000/70) (F).

associated with free methemoglobin develops at the periphery of the hematoma, in five of our six patients with stage-2 hemorrhagic neoplasms the hyperintensity appeared initially within the lesion(s), either centrally or eccentrically, rather than at the periphery (Fig. 2). It is interesting to note that the sixth patient had two stage-2 lesions, one of which exhibited central hyperintensity. In the second lesion, however, although the hyperintensity initially developed at the periphery, it was asymmetric.

Pathologic examination in all eight of the patients with stage-3 lesions demonstrated the presence of hemosiderin at the periphery of the lesion. (Fig. 6 is a histologic section obtained from the same patient whose MR is seen in Fig. 3.)

On the MR images, the hemosiderin rim appeared continuous in 10 of the lesions. In the 11th case a portion of the rim was absent between the tumor and the hemorrhage.

Seven of the 12 patients with metastatic melanoma had their lesions resected (Table 2). Three of these patients had pure stage-3 lesions, two patients had stage-1 lesions, one patient had a mixed-stage lesion with stage-3 elements, and one patient had a mixed-stage lesion without stage-3 elements. Masson and iron stains were done to determine whether the lesions contained melanin and hemosiderin. Two of the stage-3 lesions were amelanotic; all of the other lesions contained melanin. The amelanotic and melanotic lesions exhibited similar signal-intensity characteristics on MR; that
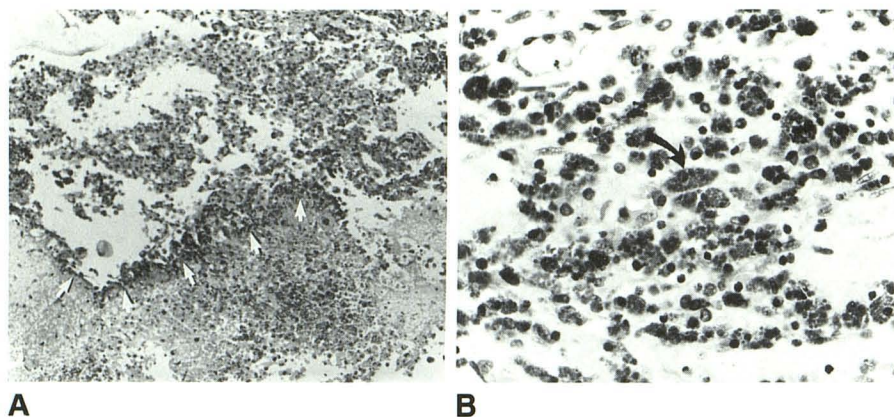
Fig. 6.—*A* and *B*, Renal cell metastasis; hemosiderin. Histologic section, obtained from patient whose CT and MR scans are seen in Fig. 3, shows rim of hemosiderin-laden macrophages at low power (*small arrows*) (*A*) and hemosiderin granules within a macrophage at high power (*curved arrow*) (*B*).

**A**　　**B**

TABLE 2: Histologically Proved Melanomas

| Case No. | Age | Gender | Metastases | Stage | Melanin | Hemosiderin | Signal Intensity | |
|---|---|---|---|---|---|---|---|---|
| | | | | | | | Short TR | Long TR |
| 1 | 49 | F | 3 | 1 | + | − | ↓ | ↓↓ |
| 2 | 50 | F | 1 | 1 | + | − | ↓ | ↓↓ |
| 3 | 45 | M | 1 | 3 | + | + | ↑↑ | ↑↑* |
| 4 | 61 | M | 2 | 3 | − | + | ↑↑ | ↑↑* |
| 5 | 54 | M | 1 | 3 | − | + | ↑↑ | ↑↑* |
| 6 | 65 | M | 1 | M (1,2) | + | − | M | M |
| 7 | 35 | M | 1 | M (1,2,3) | + | + | M | M* |

Note.—↓ = mildly hypointense, ↓↓ = markedly hypointense, ↑↑ = markedly hyperintense, * = black rim, M = mixed appearance.

is, it was not possible to distinguish between them in the presence of hemorrhage.

We also examined the stage-2, stage-3, and mixed lesions with respect to whether tumor tissue itself was visible within the lesions, and whether this was helpful in differentiating hemorrhagic neoplasms from pure hemorrhage. In 10 of the patients, there were areas within the lesions that were either isointense or slightly hypointense on the short TR images, and hyperintense on long TR images. These signal-intensity differences appeared to correlate with either nonhemorrhagic cystic areas or tumor nodularity within the hemorrhage. By definition, the stage-1 lesions were excluded because they did not contain any hyperintense areas.

Finally, the amount of edema surrounding the lesions in our patients varied. In general, the presence of edema was not helpful in differentiating hemorrhagic neoplasms from pure hemorrhage. In six of our patients, however, the amount of edema was so significant that it made the presence of underlying neoplasm more likely. In the remaining patients, we felt that the small to moderate amount of edema did not allow us to make this distinction.

## Discussion

The incidence of intracranial hemorrhage resulting from neoplasm has been reported to range from 1–14% depending on the series [16–19]. Factors that affect the incidence include the source of the clinical information (surgery vs autopsy), the type of neoplasm (primary vs secondary), and whether the patient is symptomatic [16]. Of the primary intracranial neoplasms, hemorrhage occurs most frequently in relation to pituitary neoplasms [17, 19]. Other primary tumors that have been reported to bleed include glioblastoma multiforme, lower-grade gliomas, ependymomas, choroid plexus papillomas, sarcomas, and meningiomas. The incidence of hemorrhage in metastatic neoplasms is highest in melanoma, hypernephroma, bronchogenic carcinoma, and choriocarcinoma [16, 18, 19]. Other metastatic tumors that bleed are breast and thyroid.

Delayed evolution of hemorrhage within a hemorrhagic neoplasm on MR has been reported [12]. The authors noted a delay of 16 days from the hypointensity associated with acute hemorrhage to the hyperintensity associated with the formation of free methemoglobin. We have noted even longer delays, up to several months. The etiology of this delay is unclear. Methemoglobin formation is maximal at relatively low oxygen tensions, about 20–25 mm [20, 21]. Since oxygen is necessary for the formation of the agents responsible for the oxidation of deoxyhemoglobin to methemoglobin, and oxygen limits the concentration of deoxyhemoglobin available for oxidation to methemoglobin, the formation of methemoglobin

is negligible at zero and at high oxygen tensions. At 20–25 mm, there is enough oxygen to allow formation of the reducing agents, yet not enough to limit the concentration of deoxyhemoglobin. Therefore, the relative hypoxia within tumors [22] should favor, rather than delay, the formation of methemoglobin. Perhaps a more likely explanation for the delay in evolution is the continued oozing of blood from the lesion and/or the rapid absorption of hemoglobin breakdown products by a very vascular tumor.

Since methemoglobin formation is maximal at relatively low oxygen tensions, this would appear to be the most reasonable explanation for the central hyperintensity commonly seen in our stage-2 hemorrhagic neoplasms. This is not surprising in view of the lower oxygen tension of tumors compared with normal tissue, particularly at the center of the neoplasm [22]. It also follows that in a pure hematoma, where the center has very low oxygen tension, thus inhibiting the formation of the reducing agents necessary for the oxidation of deoxyhemoglobin to methemoglobin, the formation of methemoglobin initially occurs at the periphery. In a few of our cases there were areas of hyperintensity on the short TR images that became hypointense on the long TR images (Fig. 2). This most likely represents the shortening of the T1 relaxation time by methemoglobin, and a magnetic susceptibility effect of intracellular hemoglobin breakdown products on the T2 relaxation time.

In addition to central methemoglobin formation, central hyperintensity in our hemorrhagic neoplasms also appeared to be due, in some cases, to actual visualization of tumor tissue. This could be differentiated from methemoglobin changes because the hyperintensity associated with nonhemorrhagic tumor tissue was visible only on the long TR images. The presence of nonhemorrhagic tumor foci, combined with the frequent central hyperintensity due to methemoglobin on both the short TR and long TR images, proved virtually diagnostic of hemorrhagic neoplasm.

On pathologic examination, all six of the lesions exhibiting mixed signal intensity on MR contained hemorrhage in different stages of evolution. There was a direct correlation between the pathologic and MR findings. Therefore, we believe that the mixed-intensity pattern is consistent with recurrent bleeding within the tumor.

In a report of the MR appearance of hemorrhagic neoplasms [12], the authors stated that the hemosiderin rim was absent, diminished, or irregular. Our findings were slightly different. In 10 of 11 patients with stage-3 lesions (eight of them with pathologic confirmation) the hemosiderin rim, although diminished and not as prominent as in a pure bleed, completely surrounded the hemorrhage. Whether this is a function of the size of the hemorrhage is not clear, but it is important not to exclude an underlying neoplasm if a complete rim of hemosiderin is present.

All the patients with metastatic melanoma had findings consistent with hemorrhage on MR. Although the presence or absence of melanin could not be determined on the basis of the MR appearance, the stage of evolution of the hemorrhage was correctly predicted on the basis of the MR appearance of the lesions. Therefore, it would appear that hemorrhage exerts a stronger influence on the signal characteristics than melanin. Our findings concur with a prior report [13] in which the authors found differences in the signal-intensity patterns of nonhemorrhagic melanotic melanoma, nonhemorrhagic amelanotic melanoma, and hemorrhagic melanoma, but that hemorrhagic amelanotic melanoma and hemorrhagic melanotic melanoma exhibited similar signal-intensity characteristics.

Obviously, the presence of a hemorrhage in an area not usually associated with trauma or hypertension should suggest an underlying tumor as one of the possible causes. However, tumors can also occur in locations that are more often associated with trauma or hypertension. In our study of hemorrhagic neoplasms we found certain patterns or characteristics on MR that should help the diagnostician determine the cause of a hemorrhage in any location. An underlying neoplasm should be suspected in any hemorrhage that evolves slowly, develops central or eccentric hyperintensity as it evolves, or exhibits a mixed-signal-intensity pattern. In addition, we emphasize the importance of not excluding the possibility of underlying neoplasm if the hemorrhage develops a hemosiderin rim.

REFERENCES

1. Dooms GC, Uske A, Brant-Zawadzki M, et al. Spin-echo MR imaging of intracranial hemorrhage. *Neuroradiology* **1986**;28:132–138
2. Di Chiro G, Brooks RA, Girton ME, et al. Sequential MR studies of intracerebral hematomas in monkeys. *AJNR* **1986**;7:193–199
3. Sipponen JT, Sepponen RE, Sivula A. Nuclear magnetic resonance (NMR) imaging of intracerebral hemorrhage in the acute and resolving phases. *J Comput Assist Tomogr* **1983**;7:954–959
4. Zimmerman RA, Bilaniuk LT, Grossman RI, et al. Resistive NMR of intracranial hematomas. *Neuroradiology* **1985**;27:16–20
5. Swensen SJ, Keller PL, Berquist TH, McLeod RA, Stephens DH. Magnetic resonance imaging of hemorrhage. *AJR* **1985**;145:921–927
6. Edelman RR, Johnson K, Buxton R, et al. MR of hemorrhage: a new approach. *AJNR* **1986**;7:751–756
7. Cohen MD, McGuire W, Cory DA, Smith JA. MR appearance of blood and blood products: an in vitro study. *AJR* **1986**;146:1293–1297
8. Bradley WG, Schmidt PG. Effect of methemoglobin formation on the MR appearance of subarachnoid hemorrhage. *Radiology* **1985**;156:99–103
9. Gomori JM, Grossman RI, Goldberg HI, Zimmerman RA, Bilaniuk LT. Intracranial hematomas: imaging by high-field MR. *Radiology* **1985**;157:87–93
10. Hecht-Leavitt C, Gomori JM, Grossman RI, et al. High-field MRI of hemorrhagic cortical infarction. *AJNR* **1986**;7:581–585
11. DeLaPaz RL, New PFJ, Buonanno FS, et al. NMR imaging of intracranial hemorrhage. *J Comput Assist Tomogr* **1984**;8:599–607
12. Atlas SW, Grossman RI, Gomori JM, et al. Hemorrhagic intracranial malignant neoplasms: spin-echo MR imaging. *Radiology* **1987**;164:71–77
13. Atlas SW, Grossman RI, Gomori JM, et al. MR imaging of intracranial metastatic melanoma. *J Comput Assist Tomogr* **1987**;11:577–583
14. Woodruff WW, Djang WT, McLendon RE, Heinz ER, Voorhees DR. Intracerebral malignant melanoma: high-field-strength MR imaging. *Radiology* **1987**;165:209–213
15. Sze G, Krol G, Olsen WL, et al. Hemorrhagic neoplasms: MR mimics of

occult vascular malformations. *AJNR* **1987**;8:795–802

16. Mandybur TI. Intracranial hemorrhage caused by metastatic tumors. *Neurology* **1977**;27:650–655
17. Weisberg LA. Hemorrhagic primary intracranial neoplasms: clinical-computed tomographic correlations. *Comput Radiol* **1986**;10:131–136
18. Weisberg LA. Hemorrhagic metastatic intracranial neoplasms: Clinical-computed tomographic correlations. *Comput Radiol* **1985**;9:105–114
19. Wakai S. Yamakawa K, Manaka S, Takakura K. Spontaneous intracranial

hemorrhage caused by brain tumor: its incidence and clinical significance. *Neurosurgery* **1982**;10:437–444
20. Bodansky O. Methemoglobinemia and methemoglobin-producing compounds. *Pharmacol Rev* **1951**;3:144–196
21. Neill JM, Hastings AB. The influence of the tension of molecular oxygen upon certain oxidations of hemoglobin. *J Biol Chem* **1925**;63:479–492
22. Gatenby RA, Coia LR, Richter MP, et al. Oxygen tension in human tumors: in vivo mapping using CT-guided probes. *Radiology* **1985**;156:211–214